Chain Length and Temperature Dependence of the Reversible Association of Model Acylated Proteins with Lipid Bilayers†

Chadler T. Pool‡ and Thomas E. Thompson*

Biochemistry Department, University of Virginia, Charlottesville, Virginia 22908

Received February 18, 1998; Revised Manuscript Received April 30, 1998

ABSTRACT: To study the binding of fatty-acylated proteins to lipid bilayers, we have specifically attached fatty acids to the N-terminus of chemically modified bovine pancreatic trypsin inhibitor. This was accomplished by reacting the protein with saturated fatty acid anhydrides ranging in length from 8 to 18 carbons. Following radiolabeling of the fatty-acylated proteins at Lys-15, binding of these proteins to palmitoyloleoyl phosphatidylcholine vesicles was examined as a function of temperature using ultracentrifugation to determine the fraction of bound protein. Binding of these fatty-acylated proteins exhibited a significant enthalpy change. We also examined the free-energy change of binding as a function of fatty acid chain length. Our results are complimentary to other binding studies of fatty-acylated peptides. Comparisons with other myristoylated proteins and peptides indicate that local protein structure, apart from electrostatic interactions, plays a significant role in determining the magnitude of the overall free-energy change of membrane binding of fatty-acylated proteins. Light-scattering experiments indicated that both myristoyl and palmitoyl groups can induce protein micelle formation in aqueous solution at high concentration, but that only palmitoyl groups do so at physiologically relevant concentrations. Our results support a model in which single lipid modifications are incapable of stably anchoring proteins to biological membranes but facilitate protein associations in conjunction with other modes of interaction.

The covalent attachment of palmitic, myristic, and prenyl groups to many proteins has been shown to be a modification required for their proper biological functions. Palmitoylation occurs primarily at C-terminal and N-terminal cysteine residues (*1*, *2*), although some cases of palmitoylated lysine residues have been reported (*3*). Myristoylation occurs almost exclusively at the α-amino group of N-terminal glycine residues (*4*); however, lysine residues have also been found myristoylated (*5*). The prenyl groups, farnesyl (15 carbons) and geranylgeranyl (20 carbons), are always found attached to C-terminal cysteine residues (*6*, *7*). Fatty acylation and prenylation are catalyzed by specific transferases that each specialize in the attachment of one of the groups to a specific site on the protein (*1*, *2*, *4*, *8*−*11*). In most of these systems, lipid modification of the proteins is required for correct membrane targeting. Examples of palmitoylated proteins include: all G-protein α subunits (*2*, *12*), N-Ras (*1*, *13*), Ras2, and Ha-Ras (*13*). The Ras family in addition is farnesylated. MARCKS (*14*, *15*), v-Src, and c-Src (*16*, *17*) are myristoylated, while endothelial nitric oxide synthase (eNOS) requires myristoylation and palmitoylation for targeting to caveolae on the plasma membrane (*18*, *19*).

It is clear that modification of a protein by covalent linkage of one or more lipid residues can enhance binding of the protein to a membrane through intercalation of the lipid into the membrane bilayer. The magnitude of the enhancement of binding should increase with increasing acyl or prenyl chain length. The contributions made by the different lipid modifications to the membrane binding of such proteins are important in understanding the origin of the binding energy.

Although the partitioning into bilayers of free fatty acids, both in protonated and in unprotonated forms, has been extensively studied (*4*, *20*, *21*), few studies have been carried out on biologically acylated proteins. This is due primarily to the difficulty in obtaining sufficient quantities of these proteins for binding studies and, in the case of the thioester-linked palmitoyl group, to the lability of this linkage during purification. The only relevant studies to date have involved recombinant forms of the myristoylated proteins Src (*16*) and MARCKS (*14*). From these studies it was not possible to determine the contribution made by the fatty-acid alone. Peitzsch and McLaughlin (*22*), however, have studied the binding of short, fatty-acylated peptides as well as unprotonated fatty acids. They found that the free-energy change associated with binding of a fatty-acylated peptide is the same as that of the respective free, unprotonated fatty acid, and the contribution per methylene carbon in the acyl chain is 0.825 kcal/mol. This is the same value as that cited by Tanford (*23*) obtained in studies of the partitioning of hydrocarbons between water and organic phases. Thus, the effect on binding of single amino acids or peptides two to three amino acids long to acyl chain binding is negligible. For an acylated protein, there must, however, be significant contributions to the binding free energy made by the protein itself arising from conformational and mass-dependent entropy (*24*, *25*), charge (*14*, *16*, *26*), and steric effects.

† This work was supported by NIH Grants GM-14628 and GM-23573.

* Address correspondence to this author.

‡Present address: Central Research Division, Pfizer Inc., Box 0067, Eastern Point Rd., Groton, CT 06340.

S0006-2960(98)00385-7 CCC: $15.00
Published on Web 06/23/1998

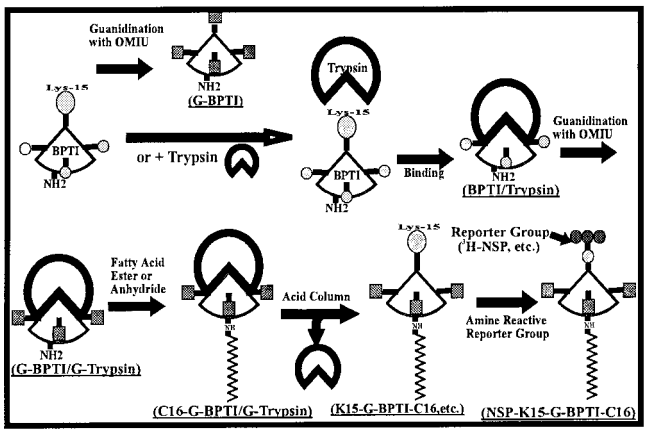

FIGURE 1: A diagram depicting the strategy employed in synthesizing the fatty-acylated proteins. Lysine residues are depicted as circles and homoarginine residues as squares. Each step in the synthesis was characterized using a C-3 reversed-phase HPLC system and/or with matrix-assisted and electrospray mass spectrometry. The names used in reference to each structure are indicated below the corresponding structures.

To examine the effect of the lipid moiety on the membrane binding of fatty-acylated proteins, we have synthesized a series of fatty-acylated proteins by attaching saturated acyl chains specifically to the N-terminus of bovine pancreatic trypsin inhibitor (BPTI)[1] using a novel derivatization scheme. This scheme, shown in Figure 1, allowed us to protect lysine-15 of BPTI with trypsin and derivatize the remaining lysine groups with *o*-methylisourea leaving the N-terminus as the only unprotected primary amine on the protein. Since native BPTI does not interact with membranes in vivo (*27*) or in vitro (*28*), we assumed that it would not contribute significantly to partitioning of the fatty-acylated proteins into phospholipid bilayers. The ability to attach fatty acids specifically at the N-terminus allowed us to compare the binding energies of different fatty acids, and since any contribution by the protein was identical in each case, it also allowed us to determine the free energy of binding per methylene carbon in each acyl chain. This study is the first in which the membrane binding of a protein has been determined as a function of fatty acid chain length and is also the first in which the free-energy change associated with membrane binding of a palmitoylated protein of any kind has been determined.

Roy et al. have shown that attachment of myristoyl and palmitoyl groups to ribonuclease A can induce the protein to form micelles in a concentration-dependent manner (*55*). To examine this phenomenon in our system, light-scattering experiments were performed using different concentrations of acylated proteins containing fatty acids from 8 to 16 carbons in length. These studies provide evidence in agreement with the findings of Roy et al. that fatty acylation can induce protein micelle formation and that the concentration range at which this occurs decreases with increasing acyl chain length.

[1] Abbreviations: BPTI, bovine pancreatic trypsin inhibitor; eNOS, endothelial nitric oxide synthase; LUV, large unilamellar vesicle; OMIU, *o*-methylisourea; POPC, palmitoyloleoyl phosphatidylcholine; G-BPTI, BPTI with all 4 lysine residues guanidinated; K15-G-BPTI, BPTI with all lysines except lysine-15 guanidinated; NSP, *N*-succinimidylpropionate.

MATERIALS AND METHODS

Materials. All lipids were purchased from Avanti Polar Lipids (Alabaster, AL). Cholesteryl-[1-^{14}C]-oleate was supplied by Amersham (Arlington Heights, IL). Ready Solv HP and Ready Safe liquid scintillation cocktails were obtained from Beckman (Palo Alto, CA), while EcoLite scintillation fluid was obtained through ICN (Costa Mesa, CA). Trizma Base, deuterium oxide, *o*-methylisourea, and type III bovine trypsin were purchased from Sigma (St. Louis, MO). Sodium chloride and ammonium bicarbonate were supplied by Aldrich (Milwaukee, WI), as were all solvents. Ammonium molybdate and the 30% solution of hydrogen peroxide were purchased from Fisher Scientific (Pittsburgh, PA), while concentrated sulfuric acid was ordered from Mallinckrodt, Inc. (Phillipsburg, NJ). Bovine pancreatic trypsin inhibitor was provided by Bayer (Kankakee, IL), and the Sephadex G-50 resin used in the gel filtration experiments was obtained from Pharmacia (Uppsala, Sweden).

Synthesis and Purification of Fatty-Acylated Proteins. The details of this synthesis will be described elsewhere (manuscript in preparation). In brief, BPTI was bound to trypsin in a one-to-one stoichiometry to protect lysine-15 of BPTI, and the resulting complex was then derivitized using *o*-methylisourea (OMIU). OMIU guanidinates the ϵ-amino groups of lysines to produce homoarginine residues, while the N-terminus remains underivatized (*29*). Following purification of the guanidinated protein complex, fatty acid anhydrides were used to specifically acylate the N-terminus of the guanidinated, trypsin-protected BPTI (K15-G-BPTI). Following dissociation of the guanidinated BPTI/trypsin complex, the fatty-acylated K15-G-BPTI was then purified on a C-3 reversed-phase HPLC column and characterized by mass spectrometry. The resulting proteins were then radio labeled at lysine-15 with tritiated *N*-succinimidylpropionate. Figure 1 shows a graphical representation of this reaction scheme.

Large Unilamellar Vesicle Preparation. Palmitoyloleoyl phosphatidylcholine (POPC) was stored at -20 °C in chloroform at concentrations of 20 or 50 mg/mL as obtained from the manufacturer. Cholesteryl-[1-^{14}C]-oleate, a nonexchangeable molecule, was added to the lipid solutions at no more than 1.5×10^{-3} mol % to serve as a means for lipid detection. To prepare vesicles, aliquots of the POPC stock solutions were transferred to test tubes and the chloroform was removed under a stream of dry nitrogen. The lipids were then placed under vacuum for 12 h or more to remove any residual solvent. Buffer was added to the dry lipids followed by vortexing to ensure complete mixing and hydration of the lipids. These suspensions of POPC were then blanketed with nitrogen and put through five freeze/thaw cycles (*30*). Following the final cycle, the resultant multilayers were transferred to a high-pressure extrusion apparatus manufactured by Lipex Biomembranes Inc. (Vancouver, BC). The lipids were next passed through two polycarbonate filters (Nucleopore; 0.1 μm pore size) a minimum of eleven times to ensure uniform vesicle size (*15*). The method of Bartlett (*31*) was used with minor modifications to determine lipid concentrations. A Beckman LS 6500 scintillation counter was used to determine the specific activities of the vesicle preparations. The dispersions of large

unilamellar vesicles (LUV) were stored under nitrogen at 4 °C.

Measuring the Binding of C12,14,16-G-BPTI to LUVs. The buffer used in all binding assays was 10 mM Tris, pH 7.5, 50 mM NaCl. This buffer was chosen to be consistent with other studies in the literature as well as to provide a system with very low absorbance in the 200−220 nm range to permit protein quantitation using these much more sensitive wavelengths (*32*).

Controls indicated that for C14-G-BPTI, approximately 4% of a 10 μM solution bound to the polyallomar tubes used for the experiments, and approximately 7% of the C16-G-BPTI bound to the tubes. Thus, to minimize the effect of this on binding to the vesicles, the acylated protein was added to LUV so that the desired free concentration of both was obtained. In all cases, the true acylated protein concentration was 10 μM. The concentration of lipid used with each of the acylated proteins was 0.1−10 mM for the C16-G-BPTI experiments, 1−100 mM for the C14-G-BPTI, and 2−200 mM with the C12-G-BPTI proteins. The total initial volume of each experiment was either 250 or 500 μL.

Once the proper dilutions had been made, the LUV/acylated protein solutions were incubated for 10−12 h at the desired temperature (10, 25, or 40 °C) in a water bath. After incubation, 50 μL aliquots were removed for scintillation counting to determine the initial concentration of acylated protein and lipid. The samples were then spun for 12 h at 45 000 rpm (relative centrifugal force = 125000*g* max, 109000*g* average) in a Beckman TL-100 tabletop ultracentrifuge equipped with a TLA-45 fixed angle rotor. Following the spin, 50 μL aliquots were removed from the supernatant, and protein concentration and any residual lipid concentration were determined by scintillation counting as described above.

As a control for the binding studies, unacylated G-BPTI, which had been radiolabeled with tritiated *N*-succinimidyl-propionate (NSP-G-BPTI), was used to determine the amount of unbound protein that spun down during the course of the experiment. Similar controls without lipid were also run with each of the acylated proteins. From these controls it was determined that a fraction of each protein spun out of solution regardless of the presence of an acyl chain. Inconsistencies in the binding data were also observed at high lipid concentrations due to the internal volume of the vesicles being inaccessible to the proteins. Corrections for both of these effects were employed and are described in Appendix A.

The partitioning of the three acylated proteins containing 16-, 14-, and 12-carbon fatty acid chains was measured at three temperatures and plotted as the fraction of acylated protein bound to lipid versus half the total lipid concentration. The reason for using half the total lipid concentration stems from the fact that the proteins cannot permeate the bilayer and therefore can only partition into the outer leaflet of the vesicles. To determine partition coefficients for each of the acylated proteins, nonlinear, least-squares fits of these data were performed using the equation

$$f_b = K_p[L]/(55.6 + K_p[L]) \quad (1)$$

Here f_b = the fraction of protein bound to vesicles; K_p = the mole fraction partition coefficient; [L] = half of the total lipid concentration (M); and 55.6 = the molar concentration of water. The data were also fit by taking the standard deviation of each data set into consideration and weighting the fits accordingly. The differences in the free energy calculated from individual weighted and unweighted curves was always less than 60 calories. The errors associated with the curves in Figure 2 were evaluated as the standard deviation of replicate observations and varied from a maximum of 20% for the low binding end of the curves to around 5% for the high binding ends. Partition coefficients and free energies reported in Table 1 were calculated from unweighted fits. By using the mole fraction partition coefficient, the cratic entropy contribution is taken into account so that the unitary Gibb's free energy change, $\Delta G_u°$, can be calculated directly (*22*). Also, since this form of the partition coefficient is independent of total solute concen-

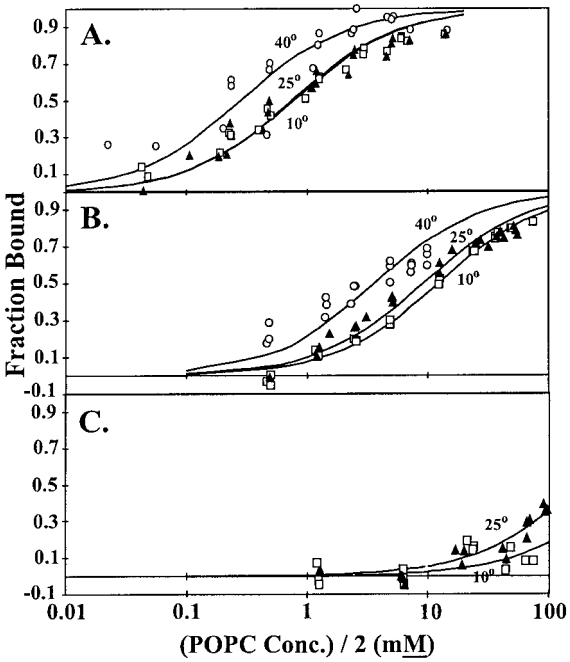

FIGURE 2: Isotherms for the binding of palmitoylated G-BPTI (C16-G-BPTI) (A), myristoylated G-BPTI (C14-G-BPTI) (B), and laurylated G-BPTI (C12-G-BPTI) (C). The fraction of acylated protein bound to POPC LUVs following ultracentrifugation of the vesicles is plotted as a function of the concentration of lipid accessible to binding (i.e. one-half the total lipid concentration). The binding experiments were performed at 40 (○), 25 (▲), and 10 (□), except for the binding of C12-G-BPTI which was not measured at 40 °C. Each data point represents an individual measurement. Note that the 25 and 10 °C curves in A are nearly indistinguishable and appear as one curve here.

Table 1: Partition Coefficients and Gibbs Free Energy Changes Calculated from Binding Isotherms (Figure 2)[a]

probe (-G-BPTI)	temperature (°C)	K_p (±)	$\Delta G_u°$, (kcal/mol) (±)
C12	10	1.7×10^2 (0.46)	−2.9 (0.14)
C12	25	3.6×10^2 (0.45)	−3.5 (0.07)
C14	10	4.5×10^3 (0.17)	−4.7 (0.02)
C14	25	6.1×10^3 (0.54)	−5.2 (0.05)
C14	40	1.5×10^4 (0.15)	−6.0 (0.05)
C16	10	7.1×10^4 (0.57)	−6.3 (0.04)
C16	25	7.4×10^4 (0.69)	−6.7 (0.05)
C16	40	2.0×10^5 (0.32)	−7.6 (0.10)

[a] Free energies were calculated using mole fraction partition coefficients and are therefore unitary Gibbs free energies.

tration, variations in protein concentration are not a concern (*33*).

In addition to these studies, experiments to assess the reversibility of binding were performed with the C12-G-BPTI and C14-G-BPTI proteins using deuterium oxide in place of water.

Dynamic Light-Scattering Measurements. Samples for light-scattering experiments were prepared by dissolving each of the HPLC purified proteins (C8,10,12,14,16-G-BPTI), along with a G-BPTI standard, in approximately 100 μL of the Tris buffer used in the binding studies. The samples were filtered using a MicroFilter apparatus (Protein Solutions, Inc.) equipped with a 20 nm Anodisc filter (Whatman) that allows filtration of samples as small as 12 μL. Dynamic light-scattering measurements were then made on each sample using a Dyna Pro-MS light-scattering apparatus (Protein Solutions, Charlottesville, VA). Samples that showed aggregate formation at their highest concentration were then systematically diluted to determine the effect of concentration on their state of aggregation. Data could only be collected for sample concentrations yielding scattering intensities greater than 15 000 photon counts/min. The final data were analyzed using the "DYNALS" software package, written by Dr. Alexander A. Goldin and Dr. Nickolay Sidorenko, to determine the particle size distribution in each sample.

Gel Filtration Experiment. To estimate the lowest concentration at which the C16-G-BPTI proteins can self-associate, gel filtration was used. In these experiments, partially fatty-acylated G-BPTI was dissolved in 5−7 mL of 50 mM ammonium bicarbonate (pH = 7.9) and loaded onto a Sephadex G-50 superfine gel filtration column (1.5 × 115 cm). The initial protein concentration loaded was 300−500 μM. Fractions were assayed for absorbance at 280 nm. Peaks indicative of protein self-association were lyophilized and re-run over the column. MALDI-TOF mass spectrometry was utilized to determine the identity and/or state of acylation of individual protein peaks.

RESULTS

Membrane Partitioning of C16,14,12-G-BPTI. Figure 2 shows the binding data for each of the proteins at different temperatures calculated using eq 1 as described in Methods, along with best-fit binding curves. Table 1 gives the partition coefficients (K_p) and binding energies ($\Delta G_u°$) calculated from these curves. Although the 10 °C curves are the best fit, it can be seen that all the curves fit the data fairly well and give small errors in K_p. There is some error in the data associated with the scintillation counting. This error was estimated at 5% for the middle of the curves and at 8% and 2% for the low and high binding portions of the curves, respectively. The underestimates of the curves at low lipid concentration and overestimates at high lipid concentration are consistent with observations made in other related binding studies (*14*, *16*, *34*) and seem to be inherent when ultracentrifugation is used to assay for reversible membrane associations. For this reason, no attempt was made to correct for such errors. An explanation of other corrections made to these data is given in Appendix A.

A few binding experiments were carried out in D_2O buffer instead of H_2O. The increased density of the D_2O solvent caused the lipid vesicles to sediment upward in the tube while the unbound, acylated proteins sedimented downward slightly. This is in contrast to sedimentation in the usual H_2O solvent in which both vesicles, and to a much lesser degree, acylated protein, sediment down the gravitational gradient. If the binding of acylated proteins to vesicles is readily reversible, then the observed binding in D_2O should be less than in H_2O due to the separation of the two species during sedimentation in D_2O. This indeed proved to be the case. Experiments with C14-G-BPTI using 130 mM lipid indicated that, following a 36 h spin in D_2O, the amount of protein associated with the vesicle pellet at the surface was reduced by a factor of 3, while C12-G-BPTI showed no observable binding at all in D_2O (data not shown).

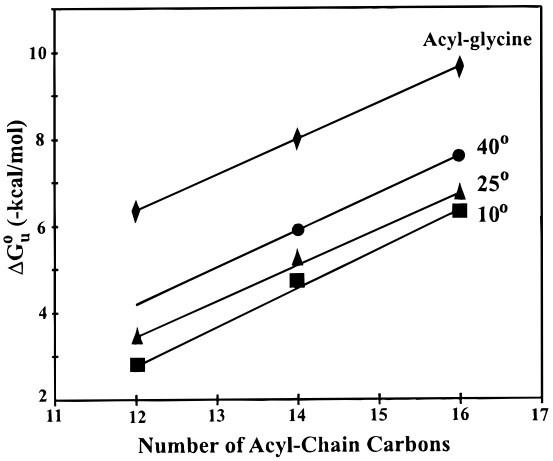

FIGURE 3: Change in $\Delta G_u°$ upon binding of fatty-acylated G-BPTI to palmitoyloleoyl phosphatidylcholine (POPC) vesicles plotted as a function of the number of carbons in the acyl chain attached to the protein. Data for the binding of acylated glycine are included for comparison (◆) (*24*). All data for acylated G-BPTI were determined from the binding isotherms in Figure 2. Plots are shown for 40 (●), 25 (▲), and 10 °C (■) experiments. The error for each data point is approximately the size of the symbol. Within error, the slope of each line is 0.85 kcal/mol per carbon in the acyl chain.

Determination of the Free Energy of Binding per Methylene Carbon. Figure 3 shows the dependence of the fatty-acylated protein binding to vesicles as a function of acyl chain length. The slopes of the curves at all temperatures are 0.8−0.85 kcal/mol. This result is in excellent agreement with the data of Peitzsch and McLaughlin (*22*) for fatty-acylated glycine partitioning into lipid bilayers and data cited by Tanford (*22*) for the partitioning of hydrocarbons between water and organic phases (*49*). Peitzsch and McLaughlin's data are included in Figure 3 for comparison. It is clear from this figure that the $\Delta G_u°$ for binding of the acylated proteins is less than that for acylated glycine.

Temperature Dependence of Membrane Partitioning. The classic hydrophobic effect predicts that the partitioning of a nonpolar solute from water to a less polar environment should result in a small enthalpic contribution dominated by a large positive entropy change (*35*−*37*) and, thus, show only a small dependence on temperature. It is interesting that between 10 and 40 °C the free energy of membrane binding increases by approximately −1.3 kcal/mol for both the C14- and C16-G-BPTI proteins (see Table 1). The partition coefficients were plotted as a function of T^{-1} as shown in Figure 4. From the Van't Hoff relation:

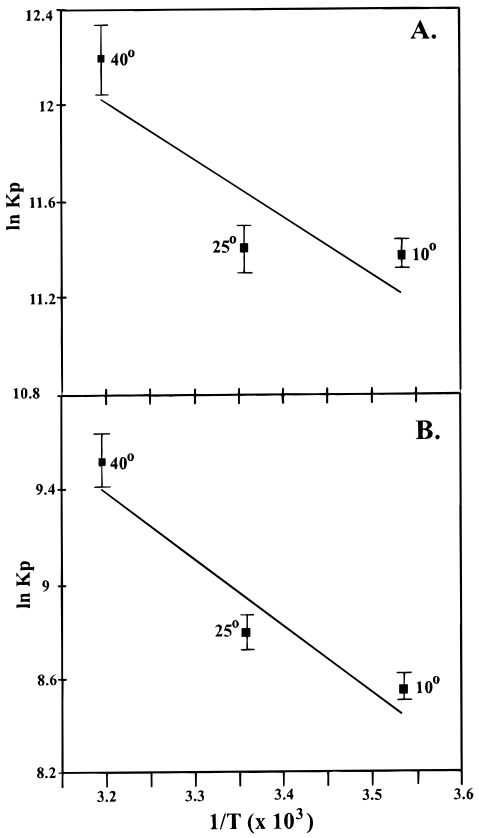

FIGURE 4: Van't Hoff plots for the temperature-dependent binding of palmitoylated G-BPTI (C16-G-BPTI) (A) and myristoylated G-BPTI (C14-G-BPTI) (B). The slopes of these lines were used to estimate the enthalpy change associated with the binding of these proteins to POPC vesicles (see eq 2). For C16-G-BPTI (A) the slope yields an enthalpy change of binding of 6 kcal/mol, while the C14-G-BPTI plot (B) gives an enthalpy change of 7 kcal/mol.

$$-\Delta H°/R = \mathrm{d}(\ln K_p)/\mathrm{d}(1/T) \qquad (2)$$

The slope defined by this plot is equal to the negative of the ratio of the enthalpy and the gas constant *R*. These plots appear to be nonlinear, however, due to the errors associated with these measurements at only 3 temperatures, considerably more data are required to unequivocally establish this feature.

The data, however, clearly do show a temperature dependence of K_p and therefore indicate a significant enthalpic contribution to the overall binding energy. To estimate roughly this contribution, a straight line was fit to the data and the slope was used to calculate $\Delta H°$ from eq 2. The C16-G-BPTI data gave a $\Delta H°$ of 6 kcal/mol and C14-G-BPTI a value of 7 kcal/mol. Assuming an average value of 6.5 kcal/mol for the enthalpy change, $\Delta S°_u$ are estimated to be 44 cal/(deg mol) for C16-G-BPTI and 39 cal/(deg mol) for C14-G-BPTI. A lower limit for $\Delta H°$ can be calculated by assuming that the $\Delta S°_u$ is the same as that found for free palmitic acid (*70*). Using this value of 34 cal/(deg mol), the enthalpy associated with the binding of C16-G-BPTI to vesicles at 25 °C is 3.4 kcal/mol. Thus, the enthalpy change for membrane binding of these acylated proteins most likely falls between 3.4 and 7 kcal/mol which is much higher than that observed for fatty acids or detergents (*36*, *38*).

Self-Association of Fatty-Acylated Proteins. Dynamic light-scattering measurements were performed at several different protein concentrations to examine the self-association of the different fatty-acylated proteins. The initial parameter determined from the scattering auto correlation function is the translational diffusion coefficient (*D*). From this, the average radius, R_h, of the hydrodynamically equivalent spherical molecule can be calculated using the Stokes−Einstein equation:

$$R_h = k_b T/(6\pi\eta D) \qquad (3)$$

Here k_b is the Boltzmann constant; *T* is absolute temperature; η is the viscosity; and *D* is the experimentally derived diffusion coefficient. The apparent molecular weight, *M*, of the acylated G-BPTI or its aggregates was then estimated from R_h by

$$M = {}^4/_3(\pi N/\upsilon)(100R_h/(f/f_o))^3 \qquad (4)$$

Where *N* is Avogadro's number; υ is the partial specific volume of BPTI; and f/f_o is the frictional ratio. Table 2 shows the hydrodynamic radii calculated using eq 3 for the concentrations accessible to measurement. Included in this table are two concentrations below 0.035 mM C16-G-BPTI determined by gel filtration. Also given in Table 2 are the molecular weights calculated at each concentration using eq 4 and from these values estimates of the aggregation numbers. A value of 0.718 mL/g was used for the partial specific volume (*39*), and a value of 1.178 was used for the frictional ratio of the monomeric proteins (*40*, *41*). The molecular weight estimate calculated using these parameters for G-BPTI monomers gave good agreement with the known value (6684). This is expected since only at much higher concentrations is there any evidence for dimer formation of BPTI (*41*, *42*). It is apparent that for C8-, C10-, and C12-G-BPTI no aggregation was observed at the concentration range studied. A 14-carbon acyl chain did, however, promote aggregation. C14-G-BPTI formed an average

Table 2: Self-Association Data for Unacylated and Fatty-Acylated G-BPTI

protein	conc (mM)[a,b]	R_h (nm)[c] (± error)	apparent MW (kDa) (± error)	apparent aggregation no.[d] (± error)
G-BPTI	0.373	1.5 ± 0.3	7.2 ± 4.3	1.1 ± 0.7
C8-G-BPTI	0.553	1.5 ± 0.3	7.2 ± 4.3	1.1 ± 0.7
C10-G-BPTI	0.592	1.5 ± 0.3	7.2 ± 4.3	1.1 ± 0.7
C12-G-BPTI	0.37	1.5 ± 0.3	7.2 ± 4.3	1.1 ± 0.7
	1.34	1.5 ± 0.3	7.2 ± 4.3	1.1 ± 0.7
	2.14	1.5 ± 0.3	7.2 ± 4.3	1.1 ± 0.7
	5.00	1.5 ± 0.1	7.2 ± 1.4	1.1 ± 0.2
C14-G-BPTI	0.14	1.9 ± 0.4	24 ± 15	3.5 ± 2.2
	0.40	2.5 ± 0.8	55 ± 53	8.0 ± 7.7
	0.60	2.6 ± 0.4	62 ± 29	9.0 ± 4.2
C16-G-BPTI	0.011[b,e]		7	1
	0.035[e]		14	2
	0.040	3.1 ± 0.6	105 ± 61	15 ± 8.7
	0.08	3.2 ± 0.7	115 ± 75	17 ± 11
	0.17	3.1 ± 0.5	105 ± 51	15 ± 7.3
	0.48	3.2 ± 0.4	115 ± 43	17 ± 6.4

[a] Protein concentrations were estimated from the scattering intensity of the samples as normalized to an unacylated G-BPTI standard. [b] Lipid binding experiments were performed at 0.01 mM protein. Note that this is below the concentration for which protein aggregation was observed for any of the acylated proteins. [c] Hydrodynamic radii were measured using dynamic light scattering. [d] Aggregation numbers were calculated using the known molecular weights of the individual proteins. [e] The two points of lowest concentration for C16-G-BPTI were estimated using gel filtration chromatography.

Table 3: Literature Values for the Free Energies of Acylated Peptides and Proteins Binding to Neutral Phospholipid Membranes

protein/peptide	lipid group[a]	temperature	ΔG_u° (kcal/mol)	reference
G-BPTI	myristoyl	25	−5.2	this study
MARCKS	myristoyl	25	−7.7	14
c-Src	myristoyl	25	−6.1	16
Gly	myristoyl	25	−8.0	22
BimTA-AC(X)R	myristoyl[b]	37	−10.6	47
G-BPTI	palmitoyl	25	−6.7	this study
Gly	palmitoyl	25	−9.6	22
BimTA-AC(X)R	palmitoyl[b]	37	−12	47
BimTA-AC(X)R	gerger[c]	37	−11	47
K-Ras (12mer)	gerger	21	−11.2	26
BimTA-AC(X)R	farnesyl[c]	37	−9.2	47
K-Ras (12mer)	farnesyl	21	−10	26

[a] All fatty acyl bonds are amide bonds except where indicated. [b] Thioester bond with cysteine. [c] Thioether bond with cysteine.

aggregate of 9 monomers at a concentration of 0.6 mM which dissociated to an aggregate of 3.5 monomers as the concentration was decreased to 0.14 mM. C16-G-BPTI formed an aggregate on average consisting of approximately 15 monomers which remained stable from 0.48 down to 0.035 mM. However, these aggregates abruptly dissociated to monomers as the concentration was decreased to 0.011 mM. Since the f/f_o value for the aggregate was unknown, f/f_o was set equal to 1 and v was taken to be the same as the monomer.

The reason for the difference in the concentration ranges examined for the different acylated proteins stems from the fact that larger aggregates scatter more light per gram of protein, and thus, the light scattering of proteins that aggregated could be measured at lower concentrations. This correlation between particle size and scattering intensity was used to estimate sample concentrations since the sample sizes were too small to obtain an absorbance at 280 nm. Since the scattering intensity of a particle increases as the sixth power of the hydrodynamic radius, the scattering intensities from each sample were normalized to that of a monomeric, G-BPTI standard of known concentration using the ratio of the sixth powers of the sample and standard, respectively. These normalized scattering intensities were then divided by the scattering intensity of the standard and multiplied by the concentration of the standard to yield the estimated concentration of each of the samples.

DISCUSSION

It is significant and interesting that the free-energy changes associated with binding of fatty-acylated G-BPTI to phosphatidylcholine vesicles in the liquid-crystalline state are substantially lower than the binding free energies of other fatty-acylated small peptides and proteins. This is easily seen by comparing the data in Table 1 for acylated G-BPTI with the data in the literature summarized in Table 3.

Since the binding energy per methylene carbon attached to BPTI (Figure 3) is the same as that observed for free fatty acids and peptides (*23*, *43*), it is apparent that the fatty acids attached to BPTI partition into the bilayer as predicted from the hydrophobic effect. Thus, the difference in binding free energy between the fatty-acylated G-BPTI and the results in Table 3 must reflect interaction of the G-BPTI with the bilayer. However, the magnitude of this interaction is very unlikely to be an intrinsic property of G-BPTI since BPTI itself has no measurable affinity for zwitterionic lipid bilayers (*28*). The obvious difference in the structure of the acylated G-BPTI proteins and biological acylated proteins such as Src and MARCKS and the acylated peptides is linkage of the acyl group to a short peptide or to a short peptide that is in turn linked to the protein moiety. It seems quite probable that the decrease in the binding of acylated G-BPTI is due to the interaction of the G-BPTI itself with the hydration layer of the bilayer surface.

Since the fatty acids are attached N-terminally directly to G-BPTI without an intervening flexible peptide segment, a substantial area of the protein and bilayer must come in close contact for complete membrane partitioning of the acyl chain. Since the G-BPTI must contact the lipid headgroups to allow the acyl chain to fully partition into the bilayer, it seems reasonable that the local membrane surface must then be substantially dehydrated, thus resulting in a positive increase in the enthalpy of binding. If the membrane surface in the immediate area of contact does not become completely dehydrated, the remaining water molecules in the hydration layer of the bilayer would be expected to sterically hinder the attached fatty acyl group from fully partitioning into the hydrophobic core of the bilayer. Assuming steric interference to be the only cause of the decreased binding, and by comparing the free-energy change associated with membrane binding of fatty-acylated G-BPTI with those of fatty-acylated amino acids, we have calculated that 3.4 methylene carbons of the attached acyl chains are prevented from partitioning into the bilayer. Although both dehydration and steric effects would decrease the membrane binding of fatty-acylated proteins, these effects would be less for membrane binding of small acylated peptides, free fatty acids, or membrane proteins, such as Src and MARCKS, that have acyl groups attached to the protein via a flexible peptide segment.

Another possibility for the observed difference in the energy of binding between acylated G-BPTI and acylated amino acids is that, in anchoring the large protein to a bilayer, the conformational entropy of the protein is decreased resulting in a decrease in the overall binding (*24*). However, since BPTI is an extremely rigid protein, this effect is likely to be small.

Russell et al. (*44*), using a carrier peptide to examine the effect of different amino acid substitutions on membrane partitioning, found that the entropy of binding increased as the hydrophobicity of the amino acid substitutions increased, but that the enthalpy change remained constant at around 4.3 kcal/mol. This indicated that the majority of the membrane partitioning enthalpy change was due to the carrier peptide and was not affected by the increase in hydrophobicity which yielded the predicted increase in entropy. This observation lends support to the interpretation of our data.

Thus, it appears that the protein itself, apart from electrostatic effects, can play a significant role in determining the overall free energy that a covalently linked fatty acid can contribute to the membrane binding of a protein. Whether the effect is steric or energetic in nature, it is clear that protein structure is a significant determinant in the magnitude of membrane partitioning of lipid-modified proteins. Further support of this conclusion is the difference in binding energies between Src and MARCKS, as well as the difference in binding energies observed between different fatty-acylated peptides (*22*, *26*, *45*−*47*). These findings,

Table 4: Sites/Types of Lipid Modifications and Basic Domains on Proteins Requiring Lipid Modifiers for Membrane Association

protein	myristoyl	palmitoyl	prenyl	basic domain	reference
$G_{q\alpha}$, $G_{11\alpha}$		C9, C10			2
$G_{s\alpha}$	*a*	C3			2
$G_{i\alpha}$, $G_{i\alpha}$	G2	C3			2
Hck	G2	C3			2
Fyn	G2	C3, C6			2
Lck	G2	C3, C5			2
ENOS	G2	C15, C26			2
H-Ras		C181, C184	C186		2
K-Ras			C186	C-terminal (8 of 10 = Lys)	6
v-Src	G2			N-terminal (5, 7, 9 = Lys)	34
$(cGMP\ dep.\ kinase)_2$	G2			N-terminal (7, 9, 12 = Lys)	54
MARCKS	G2			N-terminal (13 lysines)	14

[a] N-terminal lipid moiety detected but not characterized.

coupled with our results, show that, although the relative contribution of a lipid modification to membrane binding remains the same for a given protein or peptide, comparisons between fatty-acylated peptides and proteins must include the significant effects contributed by the local interactions at the site of acylation.

Our data, and that of others, suggest an answer to the question of why in biological systems the length of fatty acid attached to proteins is so specific, and why there are no proteins yet discovered that contain only one lipid modification as their sole means of membrane binding. Table 4 shows the sites of attachment and types of lipid modifications of most of the well-characterized proteins that are not intrinsic membrane proteins and that rely in part on lipid modifications for membrane binding. From this table it is apparent that each of these proteins has multiple lipid groups or contains a polybasic domain to facilitate membrane binding. The significance of this observation can be explained if it is assumed that the lipid concentration encountered by a protein within a cell is approximately 200 μM (*48*); it can be calculated that the free-energy change associated with binding needed to maintain 50% of a protein bound to membrane is then -7.7 kcal/mol. This value indicates that even MARCKS, with the highest free energy of binding measured for any myristoylated protein, would not be stably anchored to a membrane without additional binding contributions. It also indicates that for most proteins, such as BPTI and c-Src, it is likely that not even a palmitoyl group by itself could provide a stable anchor. This conclusion is supported by studies with free fatty acids that show half-times of desorption in the range of seconds for myristate and palmitate (*20*, *49*). Thus, it appears that none of the single-lipid modifications observed to date provide enough binding energy to stably anchor any protein to a biological membrane, although palmitoyl and geranylgeranyl groups provide significantly more binding energy than myristoyl or farnesyl groups.

These conclusions suggest a role for protein acylation in membrane targeting. In this model proposed by Gelb, and by Shahinian and Silvius (*6*, *47*), myristoyl and farnesyl groups are attached to proteins in the cytosol and allow the proteins to reversibly associate with cellular membranes. Based on our data, approximately 2% of a myristoylated protein and 21% of a palmitoylated protein would be associated with a biological membrane at equilibrium, if the binding were due only to the intercalation of an acyl group attached directly to the protein. If the target membrane possesses a palmitoyltransferase activity which selectively acylates a given protein with an additional palmitoyl group, it will become energetically trapped in that specific membrane. In the case of K-Ras, or other proteins possessing a polybasic domain, a cluster of lysine and/or arginine residues facilitates targeting and binding to the negatively charged inner leaflet of the plasma membrane. This model is supported by data on H- and N-Ras that indicate that farneslyation is required for palmitoylation to occur, and palmitoylation is required for the stable membrane binding and subsequent transforming activity of these proteins (*50*, *51*). Similar results have been obtained for endothelial nitric oxide synthase, which also displays myristoylation-dependent palmitoylation with palmitoylation required for membrane partitioning and targeting of the protein to caveolae (*18*, *19*). Gelb et al. have shown that farnesylation and methylation of Ras is required for the transferase to catalyze palmitoylation of Ras (*52*). These results suggest that the reason for myristoylation or farnesylation is to allow the modified protein to reversibly associate with membranes until a target membrane possessing a specific palmitoyltransferase or negative surface charge is encountered.

Thus, the reason for the specificity displayed by myristoyltransferase (*4*, *9*) and farnesyltransferase (*7*, *16*) for myristoyl-CoA and farnesyl-PP, respectively, stems from the weak interaction of these lipid groups with membranes. Palmitoyltransferase displays less specificity (*1*, *10*) which is reasonable since it follows that the addition of a second lipid group to trap a protein in a membrane would not be as dependent on the absolute binding energy of that single modification, and it would therefore be more efficient to use whichever group is most abundant. It has also been shown that caveolin, the signature component of caveolae, possesses a binding domain for Src tyrosine kinases, H-Ras, and eNOS (*18*, *52*). These interactions could also help to target the myristoylated and farnesylated proteins to the plasma membrane by providing increased specificity. In final support of this model, it has been shown that double lipid anchors provide anchorage of peptides to membranes with dissociation half-times on the order of tens of hours (*47*) compared to seconds for unprotonated fatty acids (*20*).

In addition to the relevance of our data to the binding of acylated proteins to bilayers, we have investigated the ability of myristoyl and palmitoyl groups to induce protein micelle formation. To date, this phenomenon has not been examined. Although studies have shown that palmitoylation facilitates the interaction of G-protein α subunits with prenylated β-γ

heterodimers (*12*), that some prenylated peptides possibly aggregate in solution (*45*), and that palmitoylation may play a role in lamin binding protein dimer formation (*53*), only one study to date has directly shown that fatty acyl groups can induce protein−protein interactions (*29*). Our data agree with the observations made by these authors that a single fatty acyl group as short as 14 carbons can induce protein−protein associations. Also of interest is the observation in both studies that the shortest fatty acid found attached to proteins, myristate, is also the shortest acyl group capable of inducing micelle formation. However, our data indicate that only palmitate can induce protein micelle formation at physiologically relevant concentrations. It may be that fatty acids are utilized by cells during initial acylation steps, since aggregation of acylated, monomeric proteins would reduce the active concentration of monomers. Our data support the notion that a function of protein fatty acylation may be to induce or facilitate protein−protein associations via interactions between acyl chains.

APPENDIX A

Corrections for Unbound Protein Spinning Down with Vesicles. Light-scattering evidence showed that some very large aggregates, very similar to those observed with chemically acylated ribonuclease A (*55*), were present in aqueous solutions of acylated G-BPTI. Attempts to remove these aggregates by ultracentrifugation in the absence of lipid vesicles failed because of the instability and minute amount of the pellet. Since the percent bound protein is calculated from the amount of protein remaining in the supernatant following centrifugation, any unbound protein that spun down with the vesicles would be measured as being bound. As an alternative to removing the aggregates, the amount of the aggregate was determined by centrifuging unacylated G-BPTI with lipid vesicles. This gave a mechanically stable pellet. As discussed in the text, there is no evidence that unacylated G-BPTI binds to phosphatidylcholine vesicles. In applying these corrections to the raw data, it was further assumed that the material in the aggregate was in equilibrium with the acylated G-BPTI so that at low concentrations of lipid the correction was maximal and decreased linearly to 0 at saturating lipid concentrations. The assumption of a reversible equilibrium between aggregates and monomers of G-BPTI was based on two observations. (1) The amount of aggregate decreased with increasing temperature. (2) The corrections improved the fit of the data to the binding isotherm and gave reasonable values of $\Delta G°$/methylene carbon. Depending upon conditions, these corrections could be as large as 24.5% at low lipid concentrations at 10 °C.

To correct the data, an estimated percent of the protein aggregates was expected to spin down and this percent of the initial protein counts was subtracted from the measured initial counts before the percent bound was calculated. To do this, the following formula was used:

$$(\text{protein counts})_{\text{corr}} = (\text{protein counts})_{\text{init}} - (1 - [\text{L}]/[\text{L}]_{\text{sat}})(C)(\text{protein counts})_{\text{init}} \quad (5)$$

where [L] = the lipid concentration for the data point; $[\text{L}]_{\text{sat}}$ = the saturating lipid concentration; and C = percent of protein assumed to spin down at 0 lipid (0.165, 0.205, 0.245 for 40, 25, and 10 °C respectively). Of course, above saturating lipid concentrations, no correction was performed. The saturating lipid concentrations for the three proteins were set at 5 mM POPC for C16-G-BPTI, 50 mM for C14-G-BPTI, and 500 mM for C12-G-BPTI. After the corrections were made, the percent bound was then simply equal to

$$1 - (\text{protein counts})_{\text{final}}/(\text{protein counts})_{\text{corr}} \quad (6)$$

Corrections for Resuspended Lipid. In all experiments at 10 and 25 °C, no more than 2% of the lipid was found remaining in the supernatant following centrifugation. However, at 40 °C, significant amounts of lipid were observed in the supernatant, presumably due to the vesicles not completely spinning down or to the pelleted vesicles resuspending during handling. Corrections were made to estimate the amount of protein that was bound to the resuspended lipid so that the amount of unbound protein could be calculated.

To make this correction, it was first necessary to determine the amount of protein associated per lipid. This was calculated by dividing the amount of corrected protein that spun out of solution by the amount of lipid that spun out of solution as defined by

$$((\text{protein counts})_{\text{corr}} - (\text{protein counts})_{\text{final}})/((\text{lipid counts})_{\text{init}} - (\text{lipid counts})_{\text{final}}) \quad (7)$$

The result from this calculation was then multiplied by the lipid counts that remained in the supernatant to yield the number of protein counts in the supernatant that were bound to vesicles that did not spin down. This amount was then subtracted from the protein counts measured in the supernatant to yield the true number of protein counts not associated with the vesicles. The fraction of protein bound to the vesicles is then defined by

$$1 - ((\text{corrected protein counts in supernatant})/(\text{corrected initial protein counts})) \quad (8)$$

Corrections for Vesicle Volume Effects. Replicate experiments performed at high lipid concentrations (over 50 mM lipid) gave inconsistent data. The inconsistencies were most pronounced at low temperature and yielded what appeared to be underestimates of the binding. The effect was almost certainly due to an increase in the total volume occupied by the vesicles. The maximum volume occupied by the vesicles can be calculated assuming the vesicles are spherical. A 100 nm spherical vesicle has an internal volume of 5.24×10^{-13} μL and approximately 160 000 lipids/vesicle. The internal volume of the vesicle will account for 2% of the total sample volume at 10 mM lipid. Thus, at 100 mM lipid, the internal volume of the vesicles will account for 20% of the total system volume. However, when the data were corrected using this assumption, the results did not correlate with observations from control experiments using unacylated proteins. This is most likely due to the fact that the vesicles do not centrifuge as flattened disks or remain completely spherical. Instead, the vesicles probably maintain some fraction of their internal volume, and it is conceivable that the amount of volume they retain may be a function of lipid concentration. Therefore, it was decided that the data from

the control experiments would be used to calculate a correction factor.

In analyzing control experiments it was observed that there was no significant change in the apparent protein concentration until lipid concentrations of 100 mM at 25 °C and 50 mM at 10 °C were reached. For lipid concentrations above this, the changes in the amount of unacylated protein that spun out of solution were assumed to be due to vesicle volume effects. These differences were observed as a decrease in the apparent amount of unacylated protein that spun out of solution, since the initial concentration of protein was underestimated due to the effect described above. Thus, the initial protein counts were increased by the percent observed in the controls. This correction was assumed to increase linearly with lipid concentration. The correction at 25 °C was calculated for lipid concentrations above 100 mM from

$$(\text{initial protein counts})_{\text{corrected}} = (\text{protein counts})_{\text{init}} + (([L]100)/100)(0.18)(\text{protein counts})_{\text{init}} + 0.02(\text{protein counts})_{\text{init}} \quad (9)$$

The correction at 10 °C was calculated for lipid concentrations above 50 mM from

$$(\text{initial protein counts})_{\text{corrected}} = (\text{protein counts})_{\text{init}} + (([L] - 50)/50)(0.1)(\text{protein counts})_{\text{init}} + 0.1(\text{protein counts})_{\text{init}} \quad (10)$$

Since these corrections are only significant for lipid concentrations above 100 mM at 25 °C and above 50 mM at 10 °C, the only data that are significantly affected are those for C12-G-BPTI binding at 10 °C. Since these corrections are approximations, especially at 10 °C the data for C12-G-BPTI binding at 10 °C must therefore be taken as a very rough approximation.

ACKNOWLEDGMENT

We wish to thank Michael Johnson for his assistance in analyzing the data.

REFERENCES

1. Schlessinger, M. J., Veit, M., and Schmidt, M. F. G. (1993) in *Lipid Modifications of Proteins* (Schlessinger, M. J., Ed.) pp 1−20, CRC Press, Boca Raton, FL.
2. Mumby, S. M. (1997) *Curr. Opin. Cell Biol. 9*, 148−154.
3. Stevenson, F. T., Bursten, S. L., Fanton, C., Locksley, R. M., and Lovett, D. H. (1993) *Proc. Natl. Acad. Sci. U.S.A. 90*, 7245−7249.
4. Duronio, R. J., Rudnick, D. A., Knoll, L. J., Johnson, D. R., and Gordon, J. I. (1993) in *Lipid Modifications of Proteins* (Schlessinger, M. J., Ed.) pp 21−58, CRC Press, Boca Raton, FL.
5. Vassilev, A. O., Plesofsk-Vig, N., and Brambl, R. (1995) *Proc. Natl. Acad. Sci. U.S.A. 92*, 8680−8684.
6. Gelb, M. H. (1997) *Science 275*, 1750−1751.
7. Casey, P. J., and Seabra, M. C. (1996) *J. Biol. Chem. 271*, 5289−5292.
8. Park, H., Boduluri, S. R., Moomaw, J. F., Casey, P. J., and Besse, L. S. (1997) *Science 275*, 1800−1804.
9. Raju, R. V., Magnuson, B. A., and Sharma, R. K. (1995) *Mol. Cell. Biochem. 149−150,* 191−202.
10. Liu, L., Dudlar, T., and Gelb, M. H. (1996) *J. Biol. Chem. 271,* 23269−23276.
11. Giannakourous, T., and Magee, A. I. (1993) in *Lipid Modifications of Proteins* (Schlessinger, M. J., Ed.) pp 135−164, CRC Press, Boca Raton, FL.
12. Wedegaertner, P. B., Wilson, P. T., and Bourne, H. R. (1995) *J. Biol. Chem. 270,* 503−506.
13. Dudler, T., and Gelb, M. H. (1996) *J. Biol. Chem. 271,* 11541−11547.
14. Kim, J., Shishido, T., Jiang, X., Aderem, A., and McLaughlin, S. (1994) *J. Biol. Chem. 269*, 28214−28219.
15. Mayer, L. D., Hope, M. J., and Cullis, P. R. (1986) *Biochim. Biophys. Acta 858*, 161−168.
16. Sigal, C. T., Zhou, W., Buser, C. A., McLaughlin, S., and Resh, M. D. (1994) *Proc. Natl. Acad. Sci. U.S.A. 91*, 12253−12257.
17. Parsons, J. T., and Weber, M. J. (1989) *Curr. Top. in Microbiol. Immunol. 146*, 79−127.
18. Shaul, P. W., Smart, E. J., Robinson, L., German, Z., Yuhanna, I. S., Ying, Y., Anderson, R. G., & Michel, T. (1996) *J. Biol. Chem. 271,* 6518−6522.
19. Robinson, L. J., and Michel, T. (1995) *Proc. Natl. Acad. Sci. U.S.A. 92*, 8680−8684.
20. Zhang, F., Kamp, F., and Hamilton, J. A. (1996) *Biochemistry 35*, 16055−16060.
21. Anel, A., Richieri, G. V., and Kleinfeld, A. M. (1993) *Biochemistry 32*, 530−536.
22. Peitzsch, R. M., and McLaughlin, S. (1993) *Biochemistry 32*, 10436−10443.
23. Tanford, C. (1980) *The Hydrophobic Effect: Formation of Micelles and Biolgoical Membranes*, pp 14−20, John Wiley & Sons, New York.
24. Silvius, J. R., and Zuckerman, M. J. (1993) *Biochemistry 32*, 3153−3161.
25. Finkelstein, A. V., and Janin, J. (1989) *Protein Eng. 3*, 1−3.
26. Ghomaschi, F., Zhang, X., Liu, L., and Gelb, M. H. (1995) *Biochemistry 34*, 11910−11918.
27. Fritz, H., and Wunderer, G. (1983) *Arzneim.-Forsch. 33*, 479−494.
28. Moll, T. S., and Thompson, T. E. (1994) *Biochemsitry 33*, 15469−15482.
29. Greenstein, J. (1935) *J. Biol. Chem. 109*, 541−544.
30. Mayer, L. D., Hope, M. J., Cullis, P. R., and Janoff. (1985) *Biochim. Biophys. Acta 817*, 193−196.
31. Bartlett, G. R. (1959) *J. Biol. Chem. 234*, 466−468.
32. Stoscheck. C. M. (1990) in *General Methods for Handling Proteins and Enzymes* (Deutscher, M. P., Ed.) pp 51−65, Academic Press, San Diego, CA.
33. Wimley, W. C., and White, S. H. (1993) *Anal. Biochem. 213*, 213-217.
34. Buser, C. A., Sigal, C. T., Resh, M. D., and McLaughlin, S. (1994) *Biochemistry 33*, 13093−13101.
35. Baldwin, R. L. (1986) *Proc. Natl. Acad. Sci. U.S.A. 83*, 8069−8072.
36. Richieri, G. V., Ogata, R. T., and Klenifeld, A. M. (1995) *J. Biol. Chem. 270,* 15076−15084.
37. Jenks, W. (1969) in *Catalysis in Chemistry and Enzymology* (Hume, D., Stork, G., King, E., Herschblach, D., and Popple, J., Eds.) pp 393−436, McGraw-Hill Book Company, New York.
38. Wenk, M. R., Alt, T., Seelig, A., and Seelig, J. (1997) *Biophys. J. 72*, 1719−1731.
39. Smith, P. E., and van Gunsteren, W. F. (1994) *J. Mol. Biol. 236*, 629−636.
40. Garcia, M. M., Jimenez, R. M. A., & Garcia, B. J. M. (1990) *Int. J. Biol. Macromol. 12*, 19−24.
41. Gallagher, W. H., and Woodward, C. K. (1989) *Biopolymers 28*, 2001−2024.
42. Zielenkiewicz, P., Georgialis, Y., and Saenger, W. (1991) *Biopolymers 31*, 1347−1349.
43. Smith, R., and Tanford, C. (1973) *Proc. Natl. Acad. Sci. U.S.A. 70*, 289−293.
44. Russell, C. J., Thorgeirsson, T. E., and Shin, Y. K. (1996) *Biochemistry 35*, 9526−9532.

45. Silvius J. R., and l'Heureux, F. (1994) *Biochemistry 33,* 3014−3022.
46. Boyartchuk, V. L., Ashby, M. N., and Rine, J. (1997) *Science 275,* 1796−1800.
47. Shahinian, S., and Silvius, J. R. (1995) *Biochemistry 34,* 3813−3822.
48. Cevc, G., and Marsh, D. (1987) *Phospholipid Bilayers: Physical Principles and Models,* John Wiley and Sons, New York.
49. Daniels, C., Noy, N., and Zakim, D. (1985) *Biochemistry 24,* 3286−3292.
50. Willumsen, B. M., Cox, A. D., Solski, P. A., Der, C. J., and Buss, J. E. (1996) *Oncogene 13,* 1901−1909.
51. Omer, C. A., and Gibbs, J. B. (1994) *Mol. Micorbiol. 11,* 219−225.
52. Li, S., Couet, J., and Lisanti, M. P. (1996) *J. Biol. Chem. 271,* 29182−29190.
53. Landowski, T. H., Drat, E. A., and Starkey, J. R. (1995) *Biochemistry 34,* 11276−11287.
54. Vaandrager, A. B., Ehlert, E. M., Jarchau, T., Lohmann, S. M., and de Jonge, H. R. (1996) *J. Biol. Chem. 271,* 7025−7029.
55. Roy, M.-O., Uppenberg, J., Robert, S., Boyer, M., Chopineau, J., and Jullien, M. (1997) *Eur. Biophys. J. 26,* 155−162.

BI980385M